Am. J. Hum. Genet. 76:42–51, 2005

Mutations within the Programmed Cell Death 10 Gene Cause Cerebral Cavernous Malformations

F. Bergametti,[1] C. Denier,[1,2] P. Labauge,[1,3] M. Arnoult,[1] S. Boetto,[4] M. Clanet,[5] P. Coubes,[6] B. Echenne,[7] R. Ibrahim,[8] B. Irthum,[9] G. Jacquet,[10] M. Lonjon,[11] J. J. Moreau,[9] J. P. Neau,[13] F. Parker,[14] M. Tremoulet,[4] E. Tournier-Lasserve,[1,2] and Société Française de Neurochirurgie

[1]INSERM E365, Faculté de Médecine Lariboisière, and [2]Laboratoire de Cytogénétique et Génétique Moléculaire, Hôpital Lariboisière, Assistance Publique-Hôpitaux de Paris, Paris; [3]Service de Neurologie, Nîmes, France; Services des [4]Neurochirurgie and [5]Neurologie, Toulouse; Services des [6]Neurochirurgie and [7]Neuropédiatrie, Montpellier, France; [8]Service de Neurochirurgie, Nantes, France; [9]Service de Neurochirurgie, Limoges, France; [10]Service de Neurochirurgie, Besançon, France; [11]Service de Neurochirurgie, Nice; [13]Service de Neurochirurgie, Poitiers, France; and [14]Service de Neurochirurgie, Kremlin-Bicêtre, France

Cerebral cavernous malformations (CCMs) are hamartomatous vascular malformations characterized by abnormally enlarged capillary cavities without intervening brain parenchyma. They cause seizures and cerebral hemorrhages, which can result in focal neurological deficits. Three CCM loci have been mapped, and loss-of-function mutations were identified in the *KRIT1* (*CCM1*) and *MGC4607* (*CCM2*) genes. We report herein the identification of *PDCD10* (programmed cell death 10) as the CCM3 gene. The *CCM3* locus has been previously mapped to 3q26-27 within a 22-cM interval that is bracketed by *D3S1763* and *D3S1262*. We hypothesized that genomic deletions might occur at the *CCM3* locus, as reported previously to occur at the *CCM2* locus. Through high-density microsatellite genotyping of 20 families, we identified, in one family, null alleles that resulted from a deletion within a 4-Mb interval flanked by markers *D3S3668* and *D3S1614*. This de novo deletion encompassed *D3S1763*, which strongly suggests that the *CCM3* gene lies within a 970-kb region bracketed by *D3S1763* and *D3S1614*. Six additional distinct deleterious mutations within *PDCD10*, one of the five known genes mapped within this interval, were identified in seven families. Three of these mutations were nonsense mutations, and two led to an aberrant splicing of exon 9, with a frameshift and a longer open reading frame within exon 10. The last of the six mutations led to an aberrant splicing of exon 5, without frameshift. Three of these mutations occurred de novo. All of them cosegregated with the disease in the families and were not observed in 200 control chromosomes. *PDCD10*, also called "*TFAR15*," had been initially identified through a screening for genes differentially expressed during the induction of apoptosis in the TF-1 premyeloid cell line. It is highly conserved in both vertebrates and invertebrates. Its implication in cerebral cavernous malformations strongly suggests that it is a new player in vascular morphogenesis and/or remodeling.

Introduction

Cerebral cavernous malformations (CCMs [MIM 116860]) are vascular malformations, mostly located within the CNS. They are characterized by abnormally enlarged capillary cavities without intervening brain parenchyma (Russel and Rubinstein 1989). The most common symptoms are seizures and neurological deficits that result from focal hemorrhages (Rigamonti et al. 1988; Labauge et al. 1998). The prevalence of this condition has been estimated to be 0.1%–0.5% (Otten et al. 1989).

Cavernous angiomas can occur in a sporadic or autosomal dominant inherited form. The proportion of familial cases has been estimated as high as 50% in Hispanic American patients with CCMs (Rigamonti et al. 1988) and close to 10%–20% in white patients (E. Tournier-Lasserve, unpublished data). Familial cases are characterized by the presence of multiple lesions, whereas sporadic cases usually harbor only one CCM lesion (Rigamonti et al. 1988; Labauge et al. 1998). Clinical penetrance is incomplete, and it has been suggested that it might depend on the CCM locus involved (Craig et al. 1998; Denier et al. 2004).

Three CCM loci have been previously mapped to 7q (*CCM1*), 7p (*CCM2*), and 3q (*CCM3*), with 40% of kindreds with CCMs being linked to *CCM1*, 20% linked to *CCM2*, and 40% linked to *CCM3* (Dubovsky et al. 1995; Craig et al. 1998). Two CCM genes have been identified so far—*KRIT1* (*CCM1*) and MGC4607 (*CCM2*)—and the nature of their mutations in patients with CCMs strongly suggests a loss of function in both

Received September 7, 2004; accepted for publication October 11, 2004; electronically published November 12, 2004.

Address for correspondence and reprints: Dr. E. Tournier-Lasserve, INSERM E365, Faculté de Médecine Lariboisière, 10, Avenue de Verdun, 75010 Paris, France. E-mail: tournier-lasserve@paris7.jussieu.fr

0002-9297/2005/7601-0005$15.00

cases (Laberge-le Couteulx et al. 1999; Sahoo et al. 1999; Liquori et al. 2003; Denier et al. 2004).

Krit1 was initially identified as a rap1A-interacting protein (Serebriiskii et al. 1997). Subsequently, its N-terminal part, which contains an NPXY motif, was shown to strongly interact with icap1α, a phosphoprotein that binds to the intracytoplasmic tail of integrin β1 (Zhang et al. 2001; Zawistowski et al. 2002). Given the multiple roles of integrins in processes such as cell differentiation, proliferation, and/or apoptosis, as well as their implications in angiogenesis, these data suggest that Krit1 might play a role in integrin signaling pathways during vessel morphogenesis. *Krit1* transcripts have been detected in neural and epithelial cells during development, and the Krit1 protein has been detected in various cells, including neurons, glial cells, and endothelial cells, and was reported to be associated with microtubules (Denier et al. 2002; Gunel et al. 2002; Guzeloglu-Kayisli et al. 2004). A recent invalidation of this gene in the mouse has shown that Krit1 is not required for vasculogenesis but is needed for arterial morphogenesis and identity (Whitehead et al. 2004). However, the early E11 embryonic lethality observed in these invalidated embryos hampered the investigations needed to explore the mechanisms that lead from Krit1 loss to CCM lesions. With regard to MGC4607, nothing is known about the function of this protein, except that it contains a phosphotyrosin-binding domain and is involved in osmolarity sensing (Uhlik et al. 2003).

The *CCM3* gene had been previously mapped to a 22-cM interval bracketed by *D3S1763* and *D3S1262*. We did not have access to any large family for which linkage analysis could be performed to reduce the size of this genetic interval. In the absence of any strong candidate gene within this large interval, we chose to use another strategy to reduce the size of the region of interest. We hypothesized that deletions might be involved in this condition, as has been reported elsewhere for other hamartomatous conditions, such as tuberous sclerosis, neurofibromatosis, or CCM2 cavernous angiomas (Viskochil et al. 1990; European Chromosome 16 Tuberous Sclerosis Consortium 1993; Trofatter et al. 1993; Denier et al. 2004). We performed a high-density microsatellite genotyping of this 22-cM interval to search for putative null alleles in 20 small but potentially informative families with CCMs. In one patient, we identified a de novo deletion within a 4-Mb interval flanked by markers *D3S3668* and *D3S1614*. This deletion encompassed *D3S1763,* the centromeric boundary of the CCM3 interval, which strongly suggests that the CCM3 gene lies within a 970-kb interval bracketed by *D3S1763* and *D3S1614*. In seven families, we identified deleterious mutations within the programmed cell death 10 gene (*PDCD10*), one of the five known genes that have been mapped to this interval. These data establish *PDCD10,* a gene highly conserved in vertebrates and invertebrates, as a new player in vessel development and/or maturation.

Material and Methods

Patients and Families

Twenty unrelated families were enrolled in this study, on the basis of three criteria: (1) each proband had at least one affected relative and/or had multiple cerebral cavernous angiomas; (2) the families of these probands were potentially informative for a study designed to detect genomic deletions, on the basis of the identification of microsatellite null alleles; and (3) molecular screening for *KRIT1* and *MGC4607* point mutations was negative. CCM diagnosis was based on cerebral magnetic resonance imaging (MRI) features and/or pathological analysis. We considered as "affected" all individuals who showed cavernous angiomas on cerebral MRI, whatever their clinical status. We considered as "healthy" all individuals with normal MRI results. Those who did not undergo MRI were classified as "unknown" (fig. 1).

DNA and RNA Extraction

Genomic DNA from probands and consenting relatives was extracted from peripheral blood by use of standard procedures. Genomic DNA from 100 unrelated, healthy, white French individuals was available as a control group. Total RNA was extracted from lymphoblastoid Epstein-Barr virus (EBV) cell lines for 17 of the 20 probands (lymphoblastoid cell lines were not available for probands C064, C077, and C114), and cDNA was prepared in accordance with standard procedures.

Genetic Markers

For the initial microsatellite screening, we used a panel of 18 microsatellite markers that spanned the CCM3 interval (*D3S1763–D3S1262*) and the immediate centromeric and telomeric regions located on both sides of this interval. The average distance between the markers was <1 Mb. This panel included markers *D3S1580, D3S3686, D3S1262, D3S3592, D3S3583, D3S3609, D3S3730, D3S3715, D3S3676, D3S3520, D3S3725, D3S3053, D3S1574, D3S1282, D3S1614, D3S3622, D3S1264,* and *D3S3673* (in qter→cen orientation) (figs. 2 and 3*A*).

Additional markers were used to define the boundaries of the de novo deletion identified in family C052, including *D3S3682, D3S3668, D3S1268, D3S3689,* and new CA-repeat markers identified through screening for dinucleotide tracks of ad hoc genomic sequences that spanned the *D3S3668–D3S1614* interval. Seven new CA-repeat markers were identified and were designated *CA-AC092965a* and *CA-AC092965b* (BAC

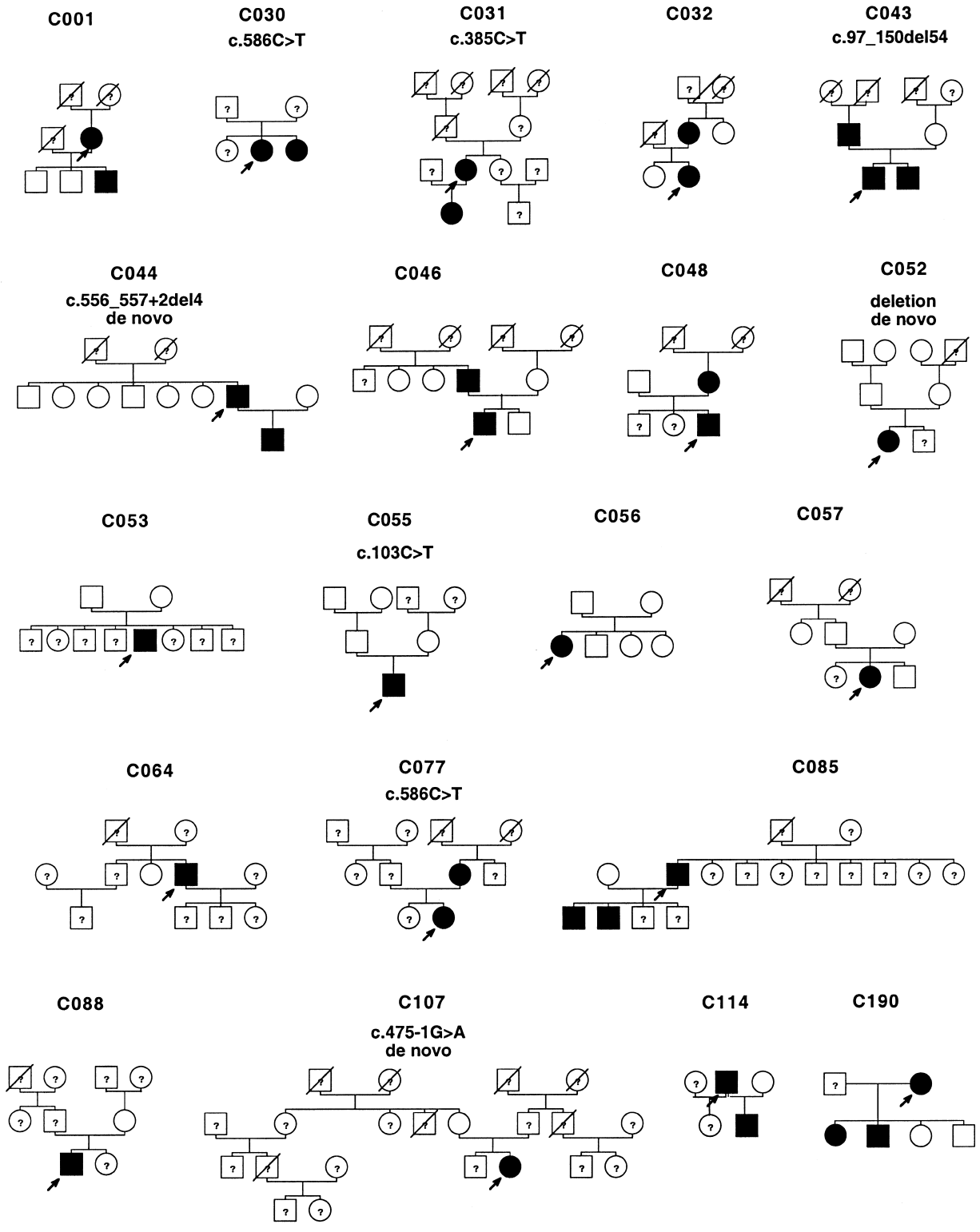

Figure 1 Genealogical trees of the 20 families with CCMs. Family numbers are indicated above each pedigree. Black symbols show affected individuals; question marks indicate unknown status; empty symbols depict healthy individuals with normal MRI results. Probands are designated by an arrow. Identified mutations have been indicated above the corresponding pedigrees.

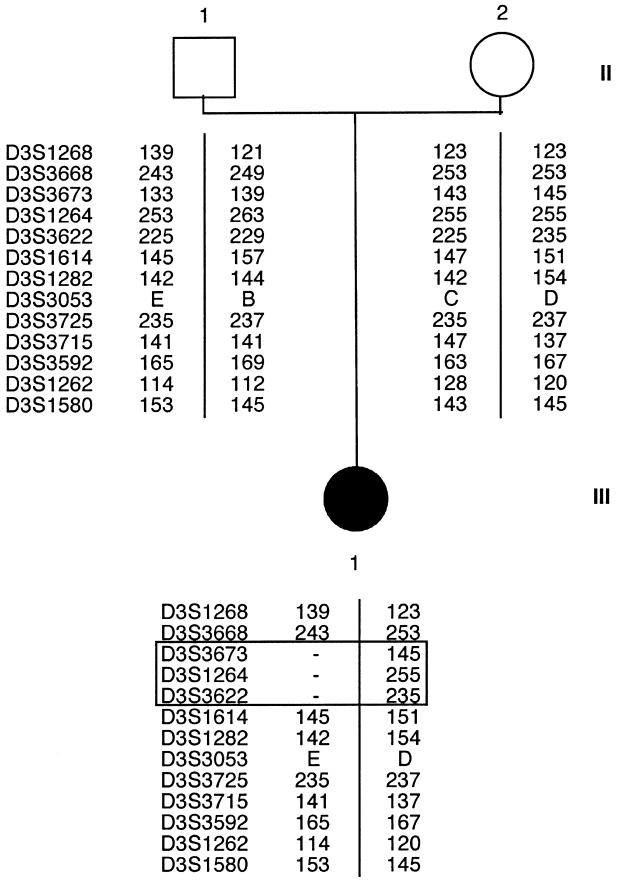

Figure 2 Parental noncontribution within family C052 at the *CCM3* locus. The genealogical tree for family C052, with CCM3 haplotypes, is shown. A null allele was detected at the *D3S3673*, *D3S1264*, and *D3S3622* markers (*boxed*), which strongly suggested the existence of a deletion; this deletion was confirmed by additional genotyping (fig. 3).

AC092965/nt 61196–61235 and nt 130628–130667), *CA-AC072046* (BAC AC072046/nt 26097–26140), *CA-AC104629a* and *CA-AC104629b* (BAC 104629/nt 92952–92991 and nt 148355–148394), *CA-AC108675* (BAC AC108675/nt 59576–59615), and *CA-AC013458* (BAC AC013458/nt 38576–38617) (fig. 3*A* and 3*B*) (see the National Center for Biotechnology Information [NCBI] Web site).

PDCD10 *Mutation Screening*

Genomic DNA of all probands was amplified using 10 sets of primers designed to amplify each of the coding exons (exons 4–10), the 5′ noncoding exons, and the flanking splice sites and was analyzed by direct sequencing on an ABI 3100 (PE Applied Biosystems) (table 1). cDNA from all probands (except probands C064, C077, and C114, from whom no cDNA was available) was amplified using a set of two primers to amplify an 802-bp fragment that spanned exons 4–10 (table 1). Amplicons were checked on agarose gels and were sequenced on an ABI 3100 (PE Applied Biosystems).

Multiple-Tissue Northern (MTN) Blot

An 802-bp cDNA probe that contained exons 4–10 was generated from a lymphoblastoid EBV cell line derived from a normal healthy control (fragment 4–10 [table 1]) and was cloned in the pGEM-T Easy Vector System (Promega). The probe sequence was identical to the reported human sequence. One hundred nanograms of the full-length cDNA fragment were radiolabeled with [^{32}P]-dCTP and were used to hybridize a human adult MTN blot (Human 12-lane MTN Blot [Clontech]) in ExpressHyb solution (Clontech) at 1–2 × 10^6 cpm/ml, in accordance with manufacturer instructions. Kodak film was exposed to the blot at −80°C for 17 h for *PDCD10* and for 6 h for the control β-actin probe (Clontech).

Results

De Novo Deletion in Family C052

None of the families available in this study was large enough to allow us to reduce the size of the *CCM3* interval through genetic linkage analysis and identification of recombinants. We hypothesized that deletions might be involved in CCM, so we searched with 18 microsatellite markers for putative null alleles in 20 unrelated families. We did not detect any abnormality, except in family C052, in whom apparent non-Mendelian inheritance was observed for three contiguous markers—*D3S3673*, *D3S1264*, and *D3S3622*—located at the centromeric boundary of the CCM3 interval (fig. 2). Patient III1 in that family appeared homozygous and failed to inherit an allele from her heterozygous unaffected father for all three markers. The same family did not exhibit incompatible genotypes with other markers, which thus eliminated inaccurate paternity information and sampling error as sources of incompatibility. Individual III1 was heterozygous at *D3S1614* and *D3S3668* and compatible with her father. Analysis of family C052 with the use of additional microsatellites located centromeric to *D3S1614* detected null alleles at *D3S3682* and *CA-AC092965b* (fig. 3), whereas genotypes of individual III1 for other centromeric markers, including *AC072046*, *AC104629*, *AC108675*, *AC013458*, and *D3S3668*, were heterozygous and compatible with the family structure. These data were consistent with a deletion of a maximum size of 1.9 Mb within an interval flanked by markers *D3S1614* (telomeric boundary) and *CA-072046* (centromeric boundary). Its minimum size was estimated at 1.1 Mb. This deletion encompassed *D3S1763*, the previously defined CCM3 centromeric

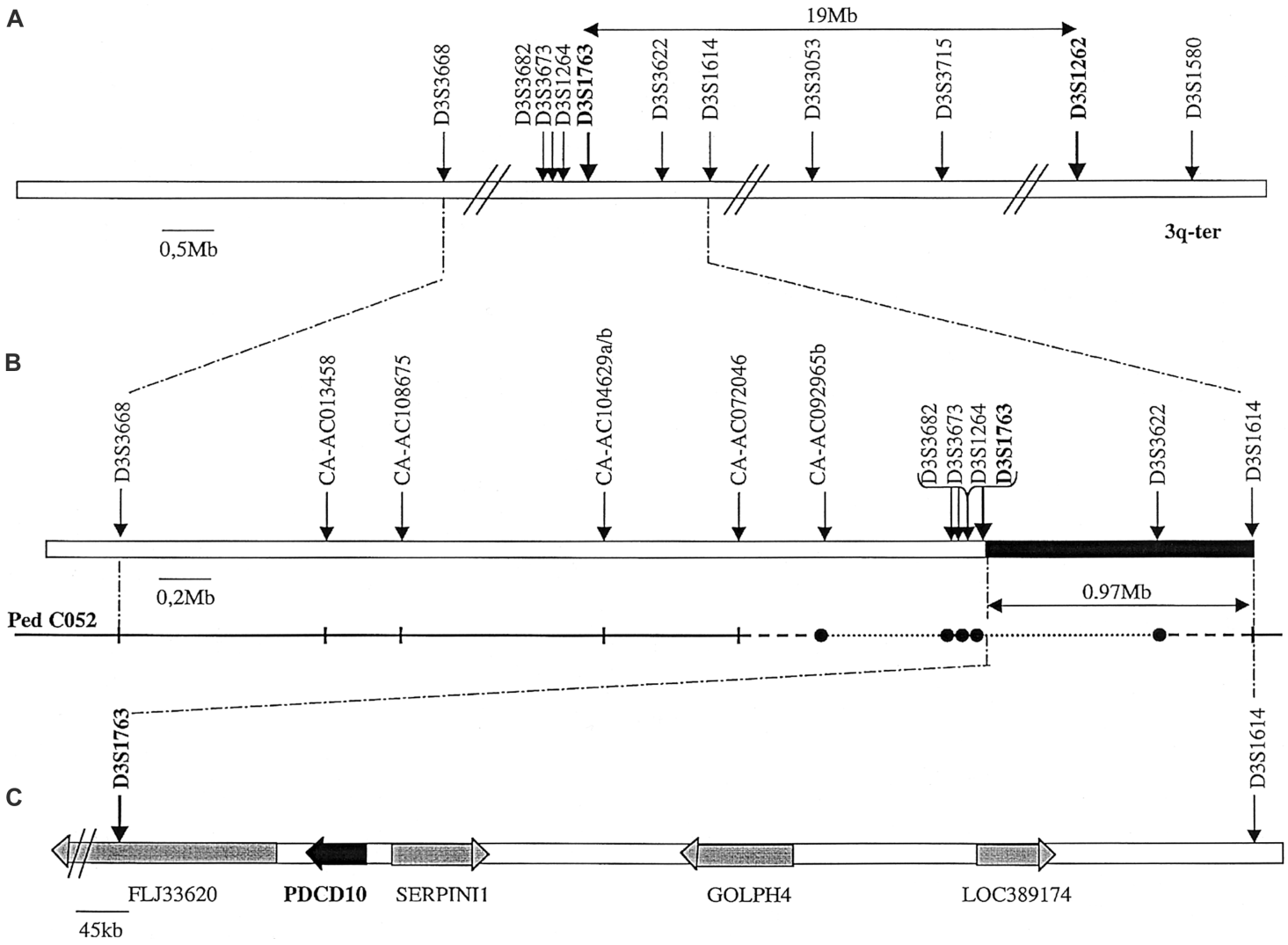

Figure 3 *A*, Genetic map of the *CCM3* locus. The two markers that bracketed the previously published CCM3 interval—*D3S1763* and *D3S1262*—are indicated in bold. Some of the microsatellite markers used to screen families for putative null alleles are shown. *B*, *CCM3* deletion in pedigree C052. Microsatellites used to identify and refine the deletion in the proband from family C052 are shown. Dots denote markers for which apparent non-Mendelian inheritance was observed in the C052 proband. Vertical bars denote heterozygosities at given markers. A de novo deletion that encompasses *D3S1763* was detected in the C052 proband. The novel critical interval, now bracketed by *D3S1763* and *D3S1614*, is blackened. *C*, Genes mapped within the novel CCM3 interval. The five genes identified within this interval are schematized as arrows.

Table 1

PCR Primers Used for Mutation Detection in the *PDCD10* Gene

Exon(s)	Oligonucleotide Sequence		Product Size (bp)
	Forward	Reverse	
1[a]	GAGTCCCCATAAGCCTCT	TTCCTCCTCCCTTTTCTCT	552
2[a]	CCCCTGCTTTGTAAGTAAGA	TAATCCCTCGGTTTCCTC	300
3[a]	AAAACTGGAAATGGAAGACA	ATTGCTTGGACCTGGAAG	453
4[a]	CCAACTAGGTTTGCTTTCAC	GCACCGATAAGAGTTCATTC	478
5[a]	CTCAGAAATGTGCTTTTTCC	AACAGGCATAAGATGGCTAA	238
6[a]	TCATGACACCTGCTTTACAA	ACAGTAGGGAAGGAAGATCC	359
7[a]	GCTAATGAATTCTGCTTTGC	GAAACCAAACGCCATAAAGT	441
8[a]	GAAGTGATTGCGCTTAACAT	CAACTAGGCATAAACCAACATC	280
9[a]	TAAAGTGCATCCCATATCCT	TGGCTAGATTAGCAACCATT	358
10[a]	ATTACCAGTCAGAACCACCA	CCTTCAGGAGGGACTGATA	400
4–10[b]	GTGAATGAAGATTCCTCTGC	CCTTCAGGAGGGACTGATA	802

[a] Genomic DNA amplification was performed for this exon with the use of PCR primers; mutation detection was done by direct sequencing. Coding exons include exons 4–10.

[b] cDNA studies were performed for these exons by the use of RT-PCR primers.

boundary, which strongly suggested that the critical interval that contained the gene spanned 970 kb and was bracketed by *D3S1763* and *D3S1614*.

PDCD10 *Point Mutations*

Five known or putative genes have been mapped within this critical interval: *FLJ33620, PDCD10, SERPINI1, GOLPH4,* and *LOC389174* (see the NCBI Web site). We designed sets of primers to amplify genomic DNA and cDNA for each of those genes. On the basis of its putative role in apoptosis, *PDCD10* was selected as the first gene for screening (Wang et al. 1999).

Genomic DNA sequence analysis identified five deleterious mutations in six of the probands, including three direct nonsense mutations and two splice-site mutations that lead to a frameshift. The probands from families C030 and C077 harbored the same mutation (nt 586C→T, stop codon at codon 196); haplotype analysis did not favor any founder effect in these two families (data not shown). The C031 proband had a mutation in exon 7 (nt 385C→T, stop codon at codon 129), and the C055 proband had a mutation in exon 5 (nt 103 C→T, stop codon at codon 35). The C107 proband had a splice-site mutation in intron 8 (nt 475-1G→A). A deletion of one of the two AAGT short repeats located between exon 9 and IVS9 was detected in the C044 proband (table 2; fig. 4*A* and 4*B*). Agarose gel electrophoresis of amplified cDNA revealed abnormal transcripts in the C107 and C044 probands. Sequence analysis of the cDNA of these probands showed an abnormal splicing of exon 9, leading to a frameshift and a change in the position of the stop codon (TGA, nt 637–639/TGA, nt 681–683).

In addition, cDNA analysis showed an abnormal transcript in which exon 5 was abnormally spliced in the C043 proband. No genomic mutation was detected at consensus splice sites in this patient. This abnormal transcript was detected neither in any of our controls nor in the >150 ESTs reported so far in databases, which strongly suggests that this abnormal transcript is pathogenic and might be due to an as-yet undetected intronic mutation that affects splicing or to a deletion of the genomic region that encompasses exon 5.

Combined haplotype and mutation screening of relatives of these probands showed that three of these mutations occurred de novo in the probands of pedigrees C044, C052, and C107. Within pedigrees C030, C031, C043, C055, and C077, the mutation cosegregated with the affected phenotype. None of the identified mutations was detected in the panel of 200 control chromosomes.

In summary, a total of eight different mutations, including one large deletion, have been observed in this panel of 20 families with CCMs. Interestingly, we did not detect any exonic polymorphism of this gene in the 20 probands.

Structure of the PDCD10 *Gene, cDNA, and Protein*

PDCD10 cDNA (alias, "*TFAR15*") was initially cloned on the basis of its up-regulated expression in a human myeloid cell line, TF-1, in which apoptosis has been induced by deprivation of granulocyte macrophage colony–stimulating factor (Wang et al. 1999). Its cDNA and genomic structures have been reported in several genome databases with >150 reported ESTs. It extends >50 kb and includes seven coding exons and three 5′ noncoding exons. Three alternative transcripts that differ only in their 5′ UTRs have been identified for this gene (GenBank accession numbers NM_007217, NM_145859, and NM_145860). The ATG initiator codon is located in the fourth exon.

Table 2

***PDCD10* Mutations**

Pedigree	Mutation[a]	Location	Effect on cDNA
C052	Deletion of the whole gene	…	…
C043	No genomic mutation detected	…	Exon 5 deletion
C055	c.103C→T	Exon 5	Nonsense mutation at codon 35
C031	c.385C→T	Exon 7	Nonsense mutation at codon 129
C107	c.475-1G→T	IVS8	Exon 9 deletion, frameshift
C044	c.556_557+2del4	Exon 9–IVS9	Exon 9 deletion, frameshift
C030	c.586C→T	Exon 10	Nonsense mutation at codon 196
C077	c.586C→T	Exon 10	Nonsense mutation at codon 196

[a] Numbering of *PDCD10* nucleotides is in accordance with the full-lengh cDNA, beginning nucleotide numbering at A of the ATG initiator codon.

The coding portion of the cDNA is 636 bp long and encodes a 212-aa predicted protein. Database searches did not identify any paralog but identified several strongly conserved orthologs both in vertebrate and invertebrate species, including *Mus musculus* (Pdcd10 [UniGene accession number Mm.316473], 98% identity at the protein level), *Danio rerio* (zgc85629, 92% identity), *Drosophila melanogaster* (CG5073, 49% identity), and *Caenorhabditis elegans* (2K896, 39% identity). In addition, partial homologous transcripts also have been reported for numerous vertebrate and invertebrate species. Searches of protein databases (ExPASy Proteomics Server) with the coding sequence of *Homo sapiens* PDCD10 did not reveal a signal peptide, transmembrane domain, or any known functional domain.

PDCD10 *mRNA Expression*

Northern blot analysis showed ubiquitous expression, in agreement with the expression pattern that can be deduced from the multiple *PDCD10* ESTs reported in the dBEST database. A band of ~1.35 kb was detected in all tissues tested, although at a different level (fig. 5), consistent with the 1.4-kb, 1.3-kb, and 1.2-kb sizes of the three reported *PDCD10* transcripts.

Discussion

We have identified *PDCD10* as the gene that causes CCM in families with CCM3, on the basis of the identification of seven distinct mutations in eight unrelated families. The nature of some of these mutations, particularly the deletion of the whole gene observed in family C052, strongly suggests that one of the mechanisms that leads to cavernous angiomas might be *PDCD10* haploinsufficiency.

We detected a mutation in 8 of the 20 families in our study. CCMs are genetically heterogeneous, and multilocus linkage data suggested that 40% of families with CCMs are linked to the *CCM3* locus (Craig et al. 1998). Since the 20 families screened in this study were included on the basis of a negative *KRIT1* (CCM1) and *MGC4607* (CCM2) mutation screening, a higher proportion of families with a *PDCD10* mutation would have been expected. Several hypotheses can be raised to explain this discrepancy. Some of these families might have a genomic deletion within either *PDCD10, KRIT1,* or *MGC4607,* which would not have been detected by the exon-by-exon sequencing approach used to screen those three genes. Another hypothesis could be the existence of additional, as-yet unidentified exons within *PDCD10*. Although this possibility cannot be excluded, there is no discrepancy between the size of the reported cDNA and that of the transcript seen in the northern blot. A third possibility is somatic mosaicism of a de novo mutation in any of the three CCM genes, which would be present at a low frequency in leukocyte DNA, particularly in the families in whom the proband is the only affected case. As has been reported elsewhere with regard to other hamartomatous conditions, this somatic mosaicism may render quite difficult the identification of the deleterious mutation (Verhoef et al. 1999). Finally, we cannot exclude the possibility of the existence of a fourth CCM gene that either was missed in the multilocus linkage analysis or is located in close proximity to one of the three CCM genes identified so far.

The identification of *PDCD10* as the CCM3 gene raises the question of its cellular function and its specific role in angiogenesis and/or remodeling of cerebral vessels. *PDCD10/TFAR15* was initially identified as a gene up-regulated in the TF-1 premyeloid cell line after growth-factor deprivation and apoptosis induction (Wang et al. 1999). This gene was shown recently to be up-regulated, in a study designed to identify apoptosis-related genes in a fibroblast cell line exposed to specific apoptosis inducers, such as staurosporine, cycloheximide, and TNF-α (Busch et al. 2004). These preliminary data suggest that this gene, which is highly conserved from nematode to human, might play a role in apoptotic pathways. Inhibition of the nematode *PDCD10* ortholog, *2K896,* leads to embryonic lethality in 40% of the embryos and a dumpy phenotype in postembryonic viable embryos (Kamath et al. 2003). However, the pathways and mechanisms that lead to these phenotypes are unknown.

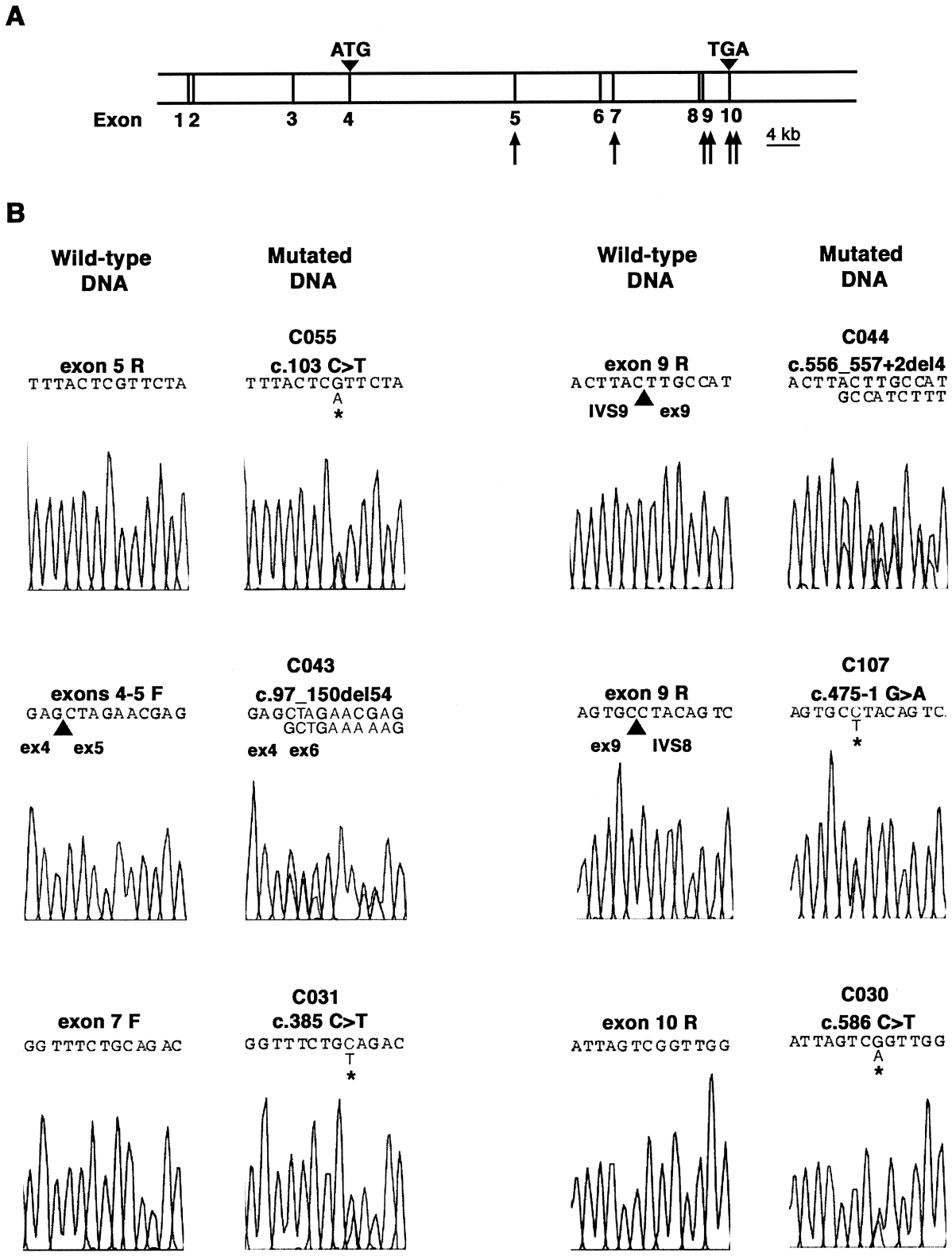

Figure 4 *PDCD10* point mutations. *A, PDCD10* genomic organization. The 10 *PDCD10* exons are numbered and are indicated by vertical hatches. The ATG initiator codon is included in the 4th exon, and the TGA stop codon is in the 10th (last) exon. The locations of the different *PDCD10* point mutations are indicated by arrows. *B,* Mutated alleles in families harboring mutations. Family numbers are given above the mutation. Sequence chromatograms of genomic DNA are shown for all probands, except for the C043 proband, whose chromatogram is of cDNA. Families C030 and C077 harbored the same mutation; therefore, we show only the chromatogram obtained in the proband of pedigree C030. F = forward primer; R = reverse primer.

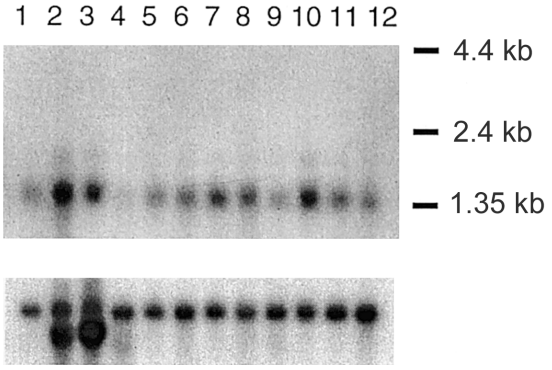

Figure 5 *PDCD10* northern blot analysis. Human adult MTN (Human 12-lane MTN Blot [Clontech]) was hybridized with a *PDCD10* (*upper panel*) and *β-actin* (*lower panel*) human cDNA probe. *Lane 1,* brain; *lane 2,* heart; *lane 3,* skeletal muscle; *lane 4,* colon; *lane 5,* thymus; *lane 6,* spleen; *lane 7,* kidney; *lane 8,* liver; *lane 9,* small intestine; *lane 10,* placenta; *lane 11,* lung; and *lane 12,* peripheral blood leukocytes.

In summary, these data establish PDCD10, a protein that has been related to apoptosis, as a new player in vessel development and/or maturation. The putative role of this protein in an apoptotic pathway that might be involved in angiogenesis and the putative link of such a pathway with either KRIT1 and/or MGC4607 remain to be investigated.

Acknowledgments

We thank all the families and all members of the Société Française de Neurochirurgie, for their participation. We are also indebted to A. Blécon, S. Goutagny, F. Marchelli, and F. Riant for previous clinical database management and *KRIT1* and *MGC4607* molecular characterization (E365 and Laboratoire de Cytogénétique, Hôpital Lariboisière, Assistance Publique-Hôpitaux de Paris). We also thank A. Joutel for excellent critical review of the study. C.D. was a Poste Accueil INSERM fellow. This work was supported by INSERM and by the Association Française contre les Myopathies (Cohortes Maladies Rares 2000), GIS Maladies Rares (AO 2002–2004), and Programme Hospitalier de Recherche Clinique Régional (PHRC AOR03031).

Electronic-Database Information

Accession numbers and URLs for data presented herein are as follows:

ExPASy Proteomics Server, http://us.expasy.org/ (for structural feature prediction)

GenBank, http://www.ncbi.nlm.nih.gov/Genbank/ (for sequence information for 3q genomic contigs and the *PDCD10* alternative transcripts [accession numbers NM_007217, NM_145859, and NM_145860])

National Center for Biotechnology Information (NCBI), http://www.ncbi.nlm.nih.gov/

Online Mendelian Inheritance in Man (OMIM), http://www.ncbi.nlm.nih.gov/Omim/ (for CCM)

UniGene, http://www.ncbi.nlm.nih.gov/UniGene/ (for *Mus musculus* Pdcd10 [accession number Mm.316473])

References

Busch CR, Heath DD, Hubberstey A (2004) Sensitive genetic biomarkers for determining apoptosis in the brown bullhead. Gene 329:1–10

Craig HD, Gunel M, Cepeda O, Johnson EW, Ptacek L, Steinberg GK, Ogilvy CS, Berg MJ, Crawford SC, Scott RM, Sabroe R, Kennedy CT, Mettler G, Beis MJ, Fryer A, Awad IA, Lifton RP (1998) Multilocus linkage identifies two new loci for a Mendelian form of stroke, cerebral cavernous malformation, at 7p15-13 and 3q25.2-27. Hum Mol Genet 7: 1851–1858

Denier C, Gasc JM, Chapon F, Domenga V, Lescoat C, Joutel A, Tournier-Lasserve E (2002) *Krit1*/cerebral cavernous malformation 1 mRNA is preferentially expressed in neurons and epithelial cells in embryo and adult. Mech Dev 117: 363–367

Denier C, Goutagny S, Labauge P, Krivosic V, Arnoult M, Cousin A, Benabid AL, et al (2004) Mutations within the *MGC4607* gene cause cerebral cavernous malformations. Am J Hum Genet 74:326–337

Dubovsky J, Zabramski JM, Kurth J, Spetzler RF, Rich SS, Orr HT, Weber JL (1995) A gene responsible for cavernous malformations of the brain maps to chromosome 7q. Hum Mol Genet 4:453–458

European Chromosome 16 Tuberous Sclerosis Consortium (1993) Identification and characterization of the tuberous sclerosis gene on chromosome 16. Cell 75:1305–1315

Gunel M, Laurans MS, Shin D, DiLuna ML, Voorhees J, Choate K, Nelson-Williams C, Lifton RP (2002) *KRIT1,* a gene mutated in cerebral cavernous malformation, encodes a microtubule-associated protein. Proc Natl Acad Sci USA 99:10677–10682

Guzeloglu-Kayisli O, Amankulor NM, Voorhees J, Luleci G, Lifton RP, Günel M (2004) KRIT1/cerebral cavernous malformation 1 protein localizes to vascular endothelium, astrocytes, and pyramidal cells of the adult human cerebral cortex. Neurosurgery 54:943–949

Kamath RS, Fraser AG, Dong Y, Poulin G, Durbin R, Gotta M, Kanapin A, Le Bot N, Moreno S, Sohrmann M, Welchman DP, Zipperlen P, Ahringer J (2003) Systematic functional analysis of the Caenorhabditis elegans using RNAi. Nature 421:231–236

Labauge P, Laberge S, Brunereau L, Levy C, Maciazek J, Tournier-Lasserve E (1998) Hereditary cerebral cavernous angiomas: clinical and genetic features in 57 French families. Lancet 352:1892–1897

Laberge-le Couteulx S, Jung HH, Labauge P, Houtteville JP, Lescoat C, Cecillon M, Marechal E, Joutel A, Bach JF, Tournier-Lasserve E (1999) Truncating mutations in *CCM1,* encoding KRIT1, cause hereditary cavernous angiomas. Nat Genet 23:189–193

Liquori CL, Berg MJ, Siegel AM, Huang E, Zawistowski JS, Stoffer T, Verlaan D, Balogun F, Hughes L, Leedom TP, Plummer NW, Cannella M, Maglione V, Squitieri F, Johnson EW, Rouleau GA, Ptacek L, Marchuk DA (2003) Mutations in a gene encoding a novel protein containing a phosphotyrosine-binding domain cause type 2 cerebral cavernous malformations. Am J Hum Genet 73:1459–1464

Otten P, Pizzolato GP, Rilliet B, Berney J (1989) 131 cases of cavernous angioma (cavernomas) of the CNS, discovered by retrospective analysis of 24,535 autopsies. Neurochirurgie 35:82–83, 128–131

Rigamonti D, Hadley MN, Drayer BP, Johnson PC, Hoenig-Rigamonti K, Knight JT, Spetzler RF (1988) Cerebral cavernous malformations: incidence and familial occurrence. N Engl J Med 319:343–347

Russel DS, Rubinstein LJ (1989) Pathology of tumors of the nervous system. 5th ed. Williams and Wilkins, Baltimore, pp 730–736

Sahoo T, Johnson EW, Thomas JW, Kuehl PM, Jones TL, Dokken CG, Touchman JW, Gallione CJ, Lee-Lin SQ, Kosofsky B, Kurth JH, Louis DN, Mettler G, Morrison L, Gil-Nagel A, Rich SS, Zabramski JM, Boguski MS, Green ED, Marchuk DA (1999) Mutations in the gene encoding KRIT1, a Krev-1/rap1a binding protein, cause cerebral cavernous malformations (*CCM1*). Hum Mol Genet 8:2325–2333

Serebriiskii I, Estojak J, Sonoda G, Testa JR, Golemis EA (1997) Association of Krev-1/rap1a with Krit1, a novel ankyrin repeat-containing protein encoded by a gene mapping to 7q21-22. Oncogene 15:1043–1049

Trofatter JA, MacCollin MM, Rutter JL, Murrell JR, Duyao MP, Parry DM, Eldridge R, Kley N, Menon AG, Pulaski K, Haase VH, Ambrose CM, Munroe D, Bove C, Haines J, Martuza RL, MacDonald ME, Sizenger BR, Short MP, Buckler AJ, Gusella JF (1993) A novel moesin-, ezrin-, radixin-like gene is a candidate for the neurofibromatosis 2 tumor suppressor. Cell 72:791–800

Uhlik MT, Abell AN, Johnson NL, Sun W, Cuevas BD, Lobel-Rice KE, Horne EA, Dell'Acqua ML, Johnson G (2003) Rac-MEKK3-MKK3 scaffolding for p38 MAPK activation during hyperosmostic shock. Nat Cell Biol 5:1104–1110

Verhoef S, Bakker L, Tempelaars AMP, Hesseling-Janssen ALW, Mazurcak T, Jozwiak S, Fois A, Bartalini G, Zonnenberg BA, van Essen AJ, Lindhout D, Halley DJ, van den Ouweland AM (1999) High rate of mosaicism in tuberous sclerosis complex. Am J Hum Genet 64:1632–1637

Viskochil D, Buchberg AM, Xu G, Cawthon RM, Stevens J, Wolff RK, Culver M, Carey JC, Copeland NG, Jenkins NA, et al (1990) Deletions and a translocation interrupt a cloned gene at the neurofibromatosis type 1 locus. Cell 62:187–192

Wang YG, Liu HT, Zhang YM, Ma DL (1999) cDNA cloning and expression of an apoptosis-related gene, human TFAR-15 gene. Science in China series C-life sciences 42:323–329

Whitehead KJ, Plummer NW, Adams J, Marchuk DA, Li DY (2004) Ccm1 is required for arterial morphogenesis: implications for the etiology of human cavernous malformations. Development 131:1437–1448

Zawistowski JS, Serebriiskii IG, Lee MF, Golemis EA, Marchuk DA (2002) KRIT1 association with the integrin-binding protein ICAP-1: a new direction in the elucidation of cerebral cavernous malformations (*CCM1*) pathogenesis. Hum Mol Genet 11:389–396

Zhang J, Clatterbuck RE, Rigamonti D, Chang DD, Dietz HC (2001) Interaction between krit1 and icap1α infers perturbation of integrin β1-mediated angiogenesis in the pathogenesis of cerebral cavernous malformation. Hum Mol Genet 10:2953–2960